ISSN 0973-8975
J.Mech.Cont.& Math. Sci., Vol.-3, No.-2, December (2008) Pages 309-323

Development of Secondary Flow and Unsteady Solutions through a Curved Duct

BY

Rabindra Nath Mondal, Md. Sharif Uddin and Md. Azmol Huda and Anup Kr. Dutta

Mathematics Discipline; Science, Engineering and Technology School, Khulna University, Khulna-9208, Bangladesh.
Tel.: 88-041-720171/Ext 265; Fax.: 88-041-731244.

E-mail: rnmondal71@yahoo.com

Abstract

In this paper, development of secondary flow and unsteady solutions through a curved duct of rectangular cross section is investigated numerically by using the spectral method. Numerical calculations are carried out for the Grashof number Gr = 1000 over a wide range of the Dean number, $0 \le Dn \le 1000$, *and the curvature* $0 < \delta \le 0.5$, *where the outer wall is heated and the inner wall is cooled. First, steady solutions are obtained by the Newton-Raphson iteration method. As a result, we obtain five branches of asymmetric steady solutions with one-, two-, four-, six-, and eight-vortex solutions at the same Dean number. Then, time evolution calculations of the unsteady solutions are performed, and it is found that the steady flow turns into chaotic flow through periodic flows, no matter what the curvature is. Finally, the complete unsteady solutions, covering the wide range of Dn and* δ, *are shown by a phase diagram.*

Keyword and phrases : *secondary flow, curved duct , chaotic flow, vortex solution.*

সংক্ষিপ্তসার

এই গবেষণা পত্রে বক্রনালীর অয়তাকার প্রস্থচ্ছেদের মধ্যদিয়ে দ্বিতীয়ক প্রবাহ এবং পরবর্তী সমাধানের বিকাশকে বর্ণালী পদ্ধতির সাহায্যে সাংখ্যমানে নির্ণয় করার জন্য অনুসন্ধান করা হয়েছে। গ্রাশফ্ সংখ্যাকে (Grashof Number), Gr = 1000, *ডীন সংখ্যার* (Dean Number), $0 \le Dn \le 1000$ *- এর বিশাল প্রসারিতায়,* $0 \le \delta \le 0.5$ *বক্রতার সাংখ্যগণনাকে পরিচালিত করা হয়েছে যখন ইহার বহিঃ প্রাচীর উত্তপ্ত এবং অন্তঃ প্রাচীর শীতল। প্রথমতঃ নিউটন - র‍্যাফ্সন* (Newton-Raphson), *পুনরাবৃত্তিমূলক পদ্ধতির সাহায্যে অপরিবর্তী সমাধান নির্ণয় করা হয়েছে। ফলস্বরূপ, একই ডীন সংখ্যায় এক -, দুই -, চার -, ছয় - এবং আট-আবর্ত সমাধান সহ অপ্রতিসম অপরিবর্তী সমাধানের পাঁচটি শাখা পাওয়া গেছে। এরপর, পরবর্তী সমাধানের ক্রমবিকশিত সময়ের গণনা করা হয়েছে এবং এটা দেখা গেছে যে বক্রতা যেমনই হউক না কেন পর্যায়কালীন প্রবাহের মধ্যে অপরিবর্তী প্রবাহ বিশৃঙ্খল প্রবাহে পরিবর্তিত হয়। পরিশেষে,* Dn *এবং* δ *-এর ব্যাপক প্রসারকে অন্তর্ভূক্তাকারে পূর্ণ পরিবর্তী সমাধানকে দশা চিত্রের সাহায্যে দেখানো হয়েছে।*

1. Introduction

The study of flows through a curved duct is of fundamental interest because of its ample applications in fluids engineering, such as in air conditioning systems, refrigeration, heat exchangers, ventilators, and the blade-to-blade passages in modern gas turbines, not to mention applications in other areas such as blood flow in veins and arteries. Such a flow is called a Dean flow and the vortices generated by it are called Dean vortices because Dean [2] was the first who formulated the problem in mathematical terms under the fully developed flow condition. He found the secondary flow consisting of a pair of counter rotating vortices caused by the centrifugal force. Since then, there have been a lot of theoretical and experimental works concerning this flow. The review articles by Berger *et al.* [1], Nandakumar and Masliyah [7] and Ito. [3] may be referred to for some outstanding reviews on curved duct flows.

One of the interesting phenomena of the flow through a curved duct is the bifurcation of the flow because generally there exist many steady solutions due to channel curvature. An early bifurcation structure and linear stability of the steady solutions for fully developed flows in a curved duct was investigated by Winters [8]. However, the existence of multiple solutions of the flow through a curved duct with the large aspect ratio was first investigated by Yanase and Nishiyama [9]. They obtained two kinds of solutions: the two-vortex solution and the four-vortex solution for the same aspect ratio. Recently, Yanase *et al.* [10] performed numerical prediction of isothermal and non-isothermal flows through a curved rectangular duct, where they obtained many branches of steady solutions and addressed the time-dependent behavior of the unsteady solutions. Very recently, Mondal *et al.* [5, 6] performed numerical prediction of isothermal and non-isothermal flows through a curved square duct, and investigated effects of curvature on the flow characteristics. However,

complete bifurcation structure as well as transient behavior of the unsteady solutions with the formation of secondary vortices are yet unresolved, which is the main objective of the present paper.

In the present paper, a numerical study is presented for the non-isothermal flow through a curved rectangular duct with differentially heated vertical sidewalls, whose outer wall is heated and the inner wall is cooled. Flow characteristics are studied over a wide range of the Dean number and the curvature by finding the steady solutions, investigating the development of secondary vortices and calculating the unsteady solutions by time evolution calculations of the resistance coefficient and the Nusselt number.

2. Basic Equations

Consider a viscous incompressible fluid through a curved duct with rectangular cross section whose width and height are $2d$ and $2h$, respectively. The aspect ratio of the duct is $\frac{h}{d}=2$. It is assumed that the outer wall of the duct is heated while the inner wall is cooled. The temperature of the outer wall is $T_0+\Delta T$ and that of the inner wall is $T_0-\Delta T$, where $\Delta T>0$. The x, y and z axes are taken to be in the horizontal, vertical, and axial directions, respectively. It is assumed that the flow is uniform in the axial direction and that it is driven by a constant pressure gradient G along the center-line of the duct, i.e., the main flow in the z-direction as shown in Fig. 1.

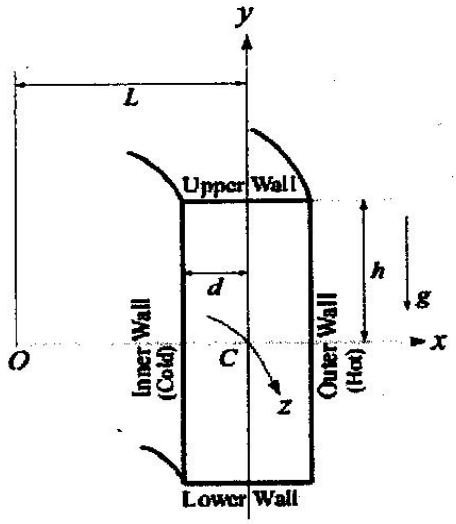

Fig. 1: Coordinate system of the curved rectangular duct.

The variables are non-dimensionalized by using of the representative length d, the representative velocity $U_0 = \nu / d$, where ν is the kinematic viscosity of the fluid. We introduce the non-dimensional variables defined as

$$u = \frac{u'}{U_0}, \quad v = \frac{v'}{U_0}, \quad w = \frac{\sqrt{2\delta}}{U_0} w', \quad T = \frac{T'}{\Delta T}, \quad t = \frac{U_0}{d} t',$$
$$\delta = \frac{d}{L}, \quad P = \frac{P'}{\rho U_0^2}, \quad G = -\frac{\partial P'}{\partial z'} \frac{d}{\rho U_0^2}.$$

where u, v and w are the non-dimensional velocity components in the x, y and z directions, respectively; t is the non-dimensional time, P the non-dimensional pressure, δ the non-dimensional curvature defined as $\delta = \frac{d}{L}$, and temperature is non-dimensionalized by ΔT. Henceforth all the variables are non-dimensionalized if not specified. Since the flow field is uniform in the z-direction, the sectional stream function ψ is introduced as follows:

$$u = \frac{1}{1+\delta x} \frac{\partial \psi}{\partial y}, \quad v = -\frac{1}{1+\delta x} \frac{\partial \psi}{\partial x} \tag{1}$$

The basic equations for w, ψ and T are derived from the Navier-Stokes equations and the heat-conduction equation with the *Boussinesq approximation* as follows:

$$(1+\delta x)\frac{\partial w}{\partial t}+\frac{1}{2}\frac{\partial(w,\psi)}{\partial(x,y)}-D_n+\frac{\delta^2}{(1+\delta x)}=(1+\delta x)\Delta_2 w-\frac{\delta}{2(1+\delta x)}\frac{\partial\psi}{\partial y}w+\delta\frac{\partial w}{\partial x}, \tag{2}$$

$$\left(\Delta_2-\frac{\delta}{1+\delta x}\frac{\partial}{\partial x}\right)\frac{\partial\psi}{\partial t}=-\frac{1}{2(1+\delta x)}\frac{\partial(\Delta_2\psi,\psi)}{\partial(x,y)}+\frac{\delta}{2(1+\delta x)^2}$$
$$\times\left[\frac{\partial\psi}{\partial y}\left(2\Delta_2\psi-\frac{3\delta}{1+\delta x}\frac{\partial\psi}{\partial x}+\frac{\partial^2\psi}{\partial x^2}\right)-\frac{\partial\psi}{\partial x}\frac{\partial^2\psi}{\partial x\partial y}\right]+\frac{\delta}{(1+\delta x)^2}\left[3\delta\frac{\partial^2\psi}{\partial x^2}-\frac{3\delta^2}{1+\delta x}\frac{\partial\psi}{\partial x}\right]$$
$$-\frac{2\delta}{(1+\delta x)}\frac{\partial}{\partial x}\Delta_2\psi+\frac{1}{2}w\frac{\partial w}{\partial y}+\Delta_2^2\psi-Gr(1+\delta x)\frac{\partial T}{\partial x}, \tag{3}$$

$$\frac{\partial T}{\partial t}+\frac{1}{2(1+\delta x)}\frac{\partial(\psi,T)}{\partial(x,y)}=\frac{1}{Pr}\left(\Delta_2 T+\frac{\delta}{1+\delta x}\right), \tag{4}$$

where $$\Delta_2\equiv\frac{\partial^2}{\partial x^2}+\frac{1}{4}\frac{\partial^2}{\partial y^2}, \quad \frac{\partial(f,g)}{\partial(x,y)}\equiv\frac{\partial f}{\partial x}\frac{\partial g}{\partial y}-\frac{\partial f}{\partial y}\frac{\partial g}{\partial x}. \tag{5}$$

Dn, *Gr* and *Pr*, which appear in Eqs. (2) - (4) are defined as

$$Dn=\frac{Gd^3}{\mu\nu}\sqrt{\frac{2d}{L}}, \quad Gr=\frac{\gamma g\Delta T d^3}{\nu^2}, \quad Pr=\frac{\nu}{\kappa}. \tag{6}$$

where μ, γ, κ and g are the viscosity, the coefficient of thermal expansion, the coefficient of thermal diffusivity and the gravitational acceleration, respectively. The rigid boundary conditions for w and ψ are

$$w(\pm1,y)=w(x,\pm1)=\psi(\pm1,y)=\psi(x,\pm1)=\frac{\partial\psi}{\partial x}(\pm1,y)=\frac{\partial\psi}{\partial y}(x,\pm1)=0, \tag{7}$$

and the conducting boundary conditions for T are assumed as

$$T(1,y)=1,\ T(-1,y)=-1,\ T(x,\pm1)=x. \tag{8}$$

In the present study, we vary *Dn* and δ while *Gr* and *Pr* are fixed as $Gr = 1000$ and $Pr = 7.0$ (water).

3. The Numerical Method

In order to solve the Eqs. (2) - (4) numerically, the spectral method is used. By this method the variables are expanded in a series of functions consisting of the Chebyshev polynomials. Details of this method are discussed by Mondal [4] and Mondal *et al.* [6]. By this method, the expansion functions $\Phi_n(x)$ and $\Psi_n(x)$ are expressed as

$$\Phi_n(x) = (1-x^2)C_n(x), \quad \Psi_n(x) = (1-x^2)^2 C_n(x), \tag{9}$$

where $C_n(x) = cos(n\,cos^{-1}(x))$ is the n-th order Chebyshev polynomial. $w(x,y,z)$, $\psi(x,y,t)$ and $T(x,y,t)$ are expanded in terms of $\Phi_n(x)$ and $\Psi_n(x)$ as

$$\left.\begin{aligned} w(x,y,z) &= \sum_{m=0}^{M}\sum_{n=0}^{N} w_{mn}(t)\Phi_m(x)\Phi_n(y), \\ \psi(x,y,t) &= \sum_{m=0}^{M}\sum_{n=0}^{N} \psi_{mn}(t)\Psi_m(x)\Psi_n(y), \\ T(x,y,t) &= \sum_{m=0}^{M}\sum_{n=0}^{N} T_{mn}(t)\Phi_m(x)\Phi_n(y) + x, \end{aligned}\right\} \tag{10}$$

where M and N are the truncation numbers in the x- and y-directions, respectively. In the present study, M=20 and N=40 have been used for sufficient accuracy of the solutions. The steady solutions are obtained by the Newton-Raphson iteration method. Then, in order to calculate the unsteady solutions, the Crank-Nicolson and Adams-Bashforth methods together with the function expansion (10) and the collocation methods are applied. In the present numerical calculations, flow characteristics are studied over a wide range of the Dean number $0 \le Dn \le 1000$ and the curvature $0 < \delta \le 0.5$ for the aspect ratio 2.

4. Resistance Coefficient and the Nusselt number

We use the resistance coefficient λ as one of the representative quantities of the flow state. It is also called the *hydraulic resistance coefficient*, and is generally used in fluids engineering, defined as

$$\frac{P_1^* - P_2^*}{\Delta z^*} = \frac{\lambda}{dh^*}\frac{1}{2}\rho\langle w^*\rangle^2, \tag{11}$$

where quantities with an asterisk denote the dimensional ones, $\langle\cdot\rangle$ stands for the mean over the cross section of the rectangular duct, and $d_h^* = 4(2d\times 4d)/(4d\times 8d)$. Since $(P_1^* - P_2^*)/\Delta z^* = G$, λ is related to the mean non-dimensional axial velocity $\langle w\rangle$ as

$$\lambda = \frac{16\sqrt{2\delta}\,Dn}{3\langle w\rangle^2}, \tag{12}$$

where $\langle w\rangle = \sqrt{2\delta}\,d/\nu\langle w^*\rangle$.

The Nusselt number, *Nu*, is defined as

$$Nu_c = \frac{1}{2}\int_{-1}^{1}\left[\frac{\delta T}{\delta x}\right]_{x=-1} dy, \quad Nu_h = \frac{1}{2}\int_{-1}^{1}\left[\frac{\delta T}{\delta x}\right]_{x=1} dy \tag{13}$$

for the steady solutions. For the unsteady solutions, on the other hand, it is defined as

$$Nu_{\tau_c} = \frac{1}{2}\int_{-1}^{1}\left\langle\left\langle\left.\frac{\delta T}{\delta x}\right|_{x=-1}\right\rangle\right\rangle dy, \quad Nu_{\tau_h} = \frac{1}{2}\int_{-1}^{1}\left\langle\left\langle\left.\frac{\delta T}{\delta x}\right|_{x=1}\right\rangle\right\rangle dy \tag{14}$$

where $\langle\langle\ \rangle\rangle$ denotes an average over a time interval τ . When the field is periodic, τ is taken as one period, and if it is chaotic τ is chosen as an appropriate time interval.

5. Results and Discussion

5.1 Steady solutions and secondary vortices

By using the path continuation technique as discussed by Mondal [4], we obtain five branches of asymmetric steady solutions for the present study. A bifurcation structure of the steady solutions is shown in Fig. 2 for Gr = 1000, δ =0.1 and 100 ≤ Dn ≤ 1000 using λ , the representative quantity of the solutions. The steady solution branches are named the *first steady solution branch* (first branch, thick solid line), the *second steady solution branch* (second branch, thin solid line), the *third steady solution branch* (third branch, dash dotdot line), the *fourth steady solution branch* (fourth branch, dashed line)

and the *fifth steady solution branch* (fifth branch, dash dotted line), respectively. It is found that the steady solution branches are independent and there exists no bifurcating relationship among them in the parameter range investigated in this paper. In this regard, it should be remarked that Yanase *et al.* [10] obtained both symmetric and asymmetric steady solutions for the isothermal flow in a curved rectangular duct. In the present study of non-isothermal flows, however, we obtain only asymmetric steady solutions. The reason is that heating the outer wall causes deformation of the secondary flow and yields asymmetry of the flow.

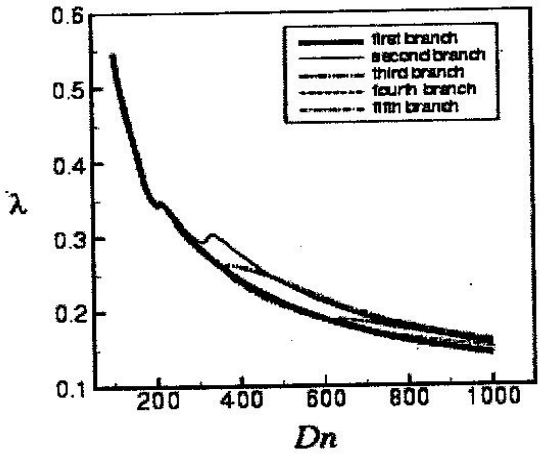

Fig. 2. Steady solution branches for $Gr = 1000$ and $100 \leq Dn \leq 1000$ at $\delta = 0.1$ (thick solid line: first branch, thin solid line: second branch, dash dotdot line: third branch, dashed line: fourth branch, dash dotted line: fifth branch).

We obtain secondary vortices on various branches and it is interesting that at the same Dean number sometimes we obtain a single-vortex or a two-vortex solution, while sometimes we obtain two-, four-, six- and eight-vortex solutions on various branches. It is found that, we obtain a single-vortex solution for $0 \leq Dn \leq 65$, two-vortex solutions for $65 < Dn \leq 245$, two- and four-vortex solutions for $245 < Dn \leq 540$, two-, four- and six-vortex solutions

for $540 < Dn \leq 855$, and two-, four-, six- and eight-vortex solutions for $855 < Dn \leq 1000$. To observe the change and development of the *secondary vortices*, also called the *Dean vortices*, contours of secondary flow and temperature profile are shown in Fig. 3 for Dn=50, 175, 500, 800 and 950, for example, where in the figures of the secondary flow, solid lines ($\psi \geq 0$) show that the secondary flow is in the counter clockwise direction while the dotted lines ($\psi < 0$) in the clockwise direction. Similarly, in the figures of the temperature field, solid lines are those for $T \geq 0$ and dotted ones for $T < 0$. As seen in Fig. 3, the secondary flow is a one-, two-, four-, six- and eight-vortex solutions at the same Dean number which are asymmetric with respect to the horizontal center plane $y = 0$. The formation of secondary vortices at various Dn is also shown by a phase diagram in Fig. 4.

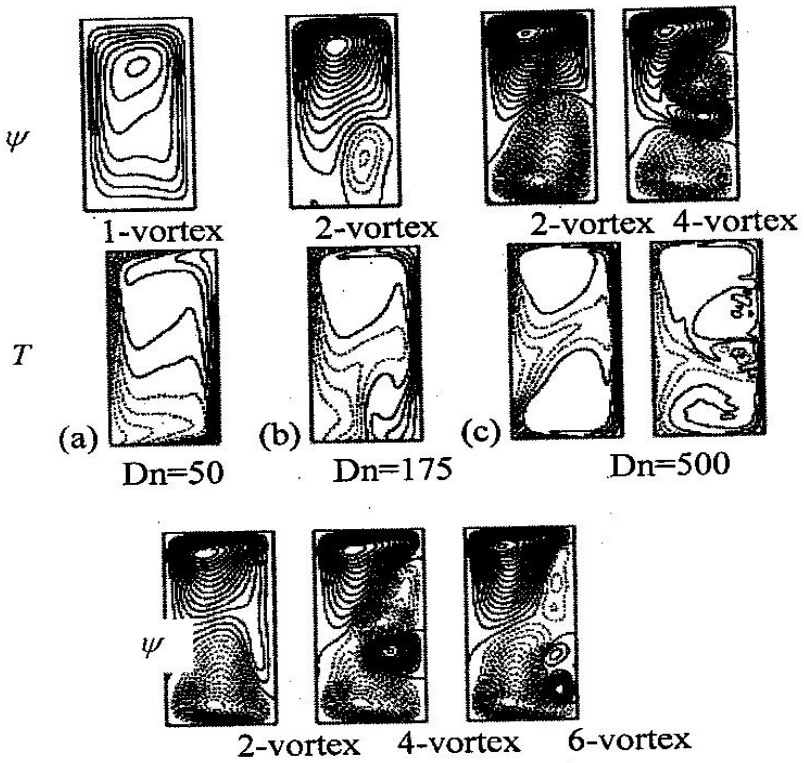

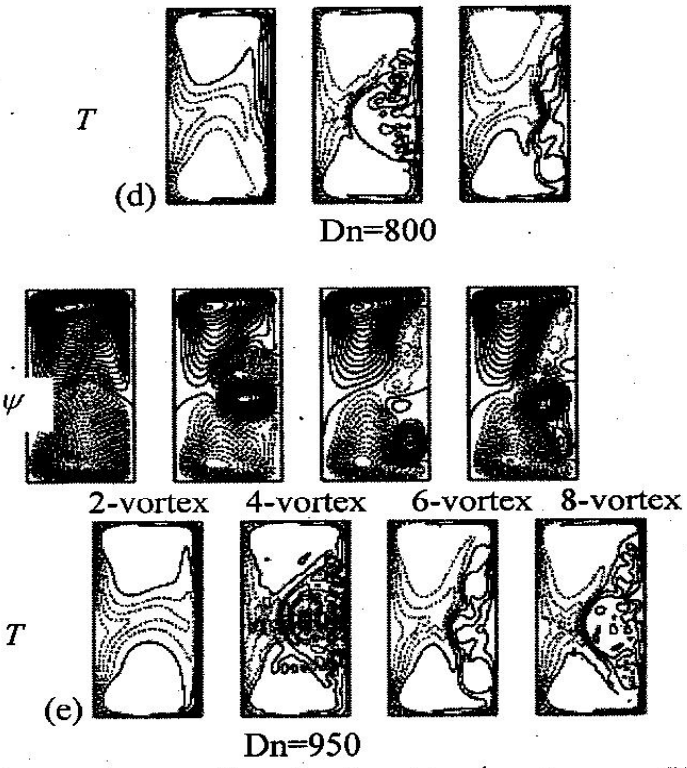

Fig. 3. Contours of secondary vortices (top) and temperature profile (bottom) at various *Dn.* (a) *Dn* = 50, (b) Dn=175, (c) Dn=500, (d) Dn=800 and (e) Dn=950.

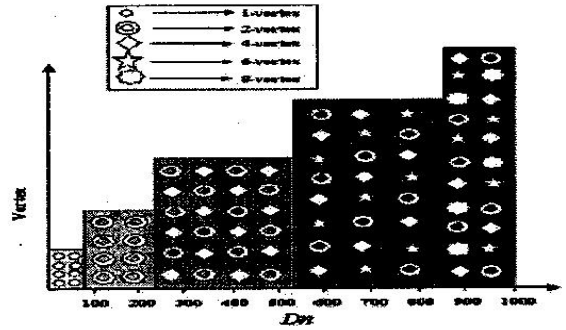

Fig. 4. Phase diagram of the secondary vortices for *Gr* = 1000 and δ =0.1.

5.2 Unsteady solutions

In order to study the nonlinear behavior of the unsteady solutions, time evolution calculations are performed for $0 \le \mathrm{Dn} \le 1000$ and $0 < \delta \le 0.5$ at Gr=1000. We perform time-evolution calculations of λ and Nu at various Dn. In this paper, unsteady solutions for δ =0.1 are discussed in detail, and then

complete unsteady solutions, covering the wide range of Dn and δ investigated in this paper, are shown by a phase diagram.

Time evolutions of λ are performed for Dn=50, 100, 300, 500 and 1000 as shown in Fig. 5. It is found that the flow becomes steady state at Dn=50 but periodic for Dn=100. However, the flow ceases to be steady state once again at Dn=300 but periodic for Dn=500 and finally chaotic at Dn=1000. In order to be certain whether the flow is periodic or chaotic at Dn=100, 500 and 1000, we then perform time-evolutions Nu at the same Dn.

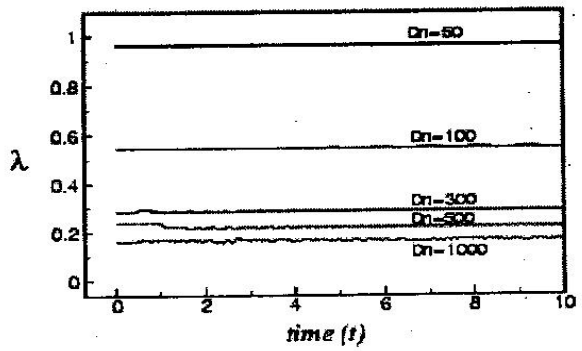

Fig. 5: Time-evolution of λ for Gr = 1000 at Dn = 50, 100, 300, 500 and 1000.

Figure 6(a) shows time-evolution of Nu for Dn=300 and it is clearly seen that the flow is periodic. Contours of typical secondary flow and temperature profile for Dn=300 are shown in Fig. 6(b), for one period of oscillation, where it is seen that secondary flow is a two-vortex solution with one large vortex dominating the other one. We then perform time-evolutions of Nu for Dn=500 and Dn=1000 as shown in Figs. 7(a) and 8(a), respectively. It is found that the flow is periodic at Dn=500 but chaotic for Dn=1000. To observe the change of the flow characteristics, as time proceeds, contours of secondary flow and temperature profile for Dn=500 and Dn=1000 are shown in Figs. 7(b) and 8(b) respectively, where it is seen that the secondary flow is a two-vortex solution for Dn=500 but four-vortex solution for Dn=1000.

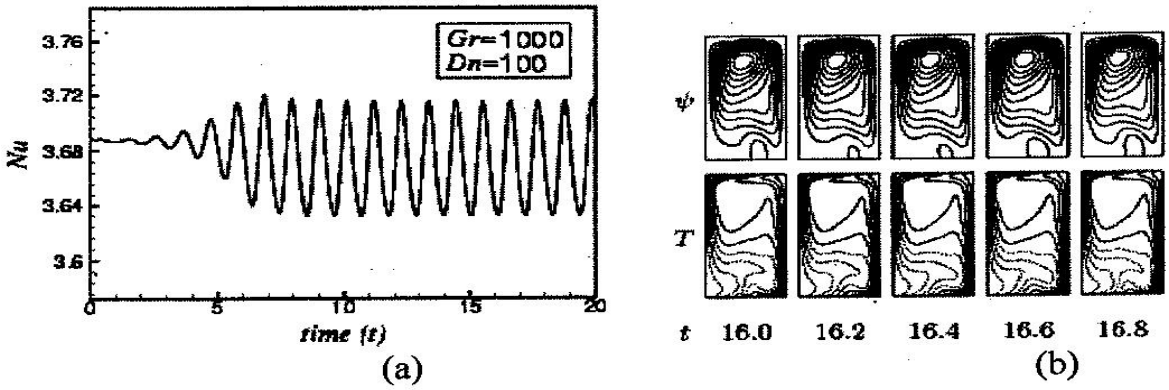

Fig. 6. Time-evolution of the Nusselt number (Nu) for $Dn = 100$.

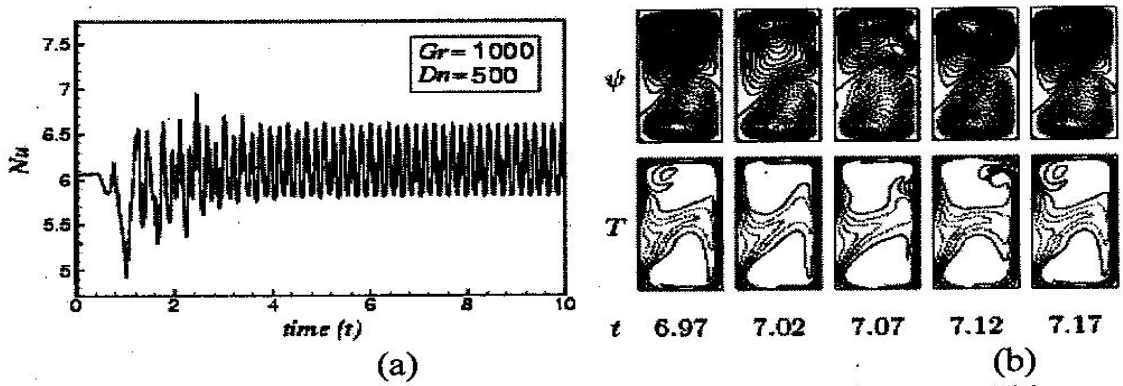

Fig. 7. Time-evolution of the Nusselt number (Nu) for $Dn = 500$.

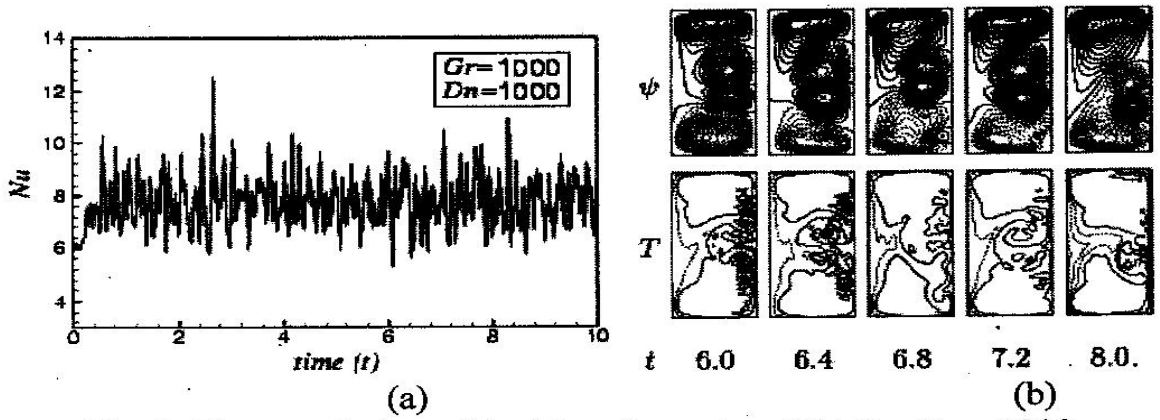

Fig. 8. Time-evolution of the Nusselt number (Nu) for $Dn = 1000$.

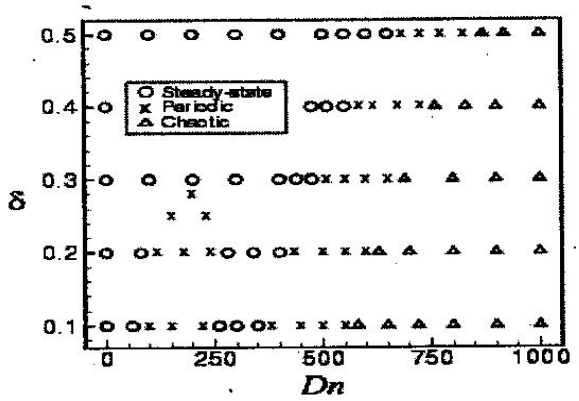

Fig. 9. Distribution of the time-dependent solutions in the Dn-δ plane for $0 \le Dn \le 1000$ and $0 < \delta \le 0.5$.

Finally, time evolution computations for other values of δ are performed and presented by a phase diagram in Fig. 9 in the Dean number versus curvature (Dn-δ) plane for $0 \le Dn \le 100$ and $0 < \delta \le 0.5$. In this figure, the circles indicate stable steady solutions, the crosses periodic solutions and the triangles chaotic solutions. As seen in Fig. 9, the steady flow turns into chaotic flow through periodic flows. However, for $\delta < 0.28$, the period solution occurs in two different intervals of the Dean number and the flow undergoes in the scenario '*steady* → *periodic* → *steady* → *periodic* → *chaotic*', if Dn is increased. If δ increased further ($\delta \ge 0.28$), the flow characteristics remain a change and the flow undergoes '*steady* → *periodic* → *chaotic*', if Dn is increased. It is found that as δ increases the region of stable steady solution increases and consequently the region of periodic state and hence the chaotic state is delayed.

6. Conclusions

In this paper, a numerical study is presented for the non-isothermal flow through a curved rectangular duct with differentially heated vertical sidewalls whose outer wall is heated and the inner wall is cooled. Numerical calculations are carried out over a wide range of the Dean number and the curvature by

using the spectral method. We obtain five branches of asymmetric steady solutions with multi-vortex solutions. It is found that there exist one-, two-, four-, six- and eight-vortex solutions at the same Dean number.

Time-evolution calculations of the unsteady solutions show that the steady flow turns into periodic first and then chaotic if *Dn* is increased, no matter what the curvature is. However, for δ <0.28, the period solution occurs in two different intervals of the Dean number and the flow undergoes in the scenario '*steady* → *periodic* → *steady* → *periodic* → *chaotic*', if Dn is increased. For larger δ ($\delta \geq 0.28$), on the other hand, the flow undergoes '*steady* → *periodic* → *chaotic*', if Dn is increased. It is found that as δ increases the region of stable steady solution increases and consequently the region of periodic state and hence the chaotic state is delayed. It is also found that the chaotic solution occurs at larger Dean numbers if the curvature becomes large.

References

1) Berger, S. A., Talbot, L. and Yao, L. S., Flow in curved pipes, Annual Review of Fluid Mechanics, Vol. **35,** pp. 461–512, 1983.

2) Dean, W. R., Note on the motion of fluid in a curved pipe, Philosophical

3) Ito, H., Flow in curved pipes, JSME International Journal, Vol. **30,** pp. 543–552, 1987.

4) Mondal, R. N. 2006. Isothermal and non-isothermal flows through curved ducts with square and rectangular cross sections, Ph.D. Thesis, Department of Mechanical Engineering, Okayama University, Japan.

5) Mondal, R. N.; Kaga, Y.; Hyakutake, T. and Yanase, S., Effects of curvature and convective heat transfer in curved square duct flows, Trans. ASME, Journal of Fluids Engineering, Vol. **128(9),** pp. 1013–1023, 2006.

6) Mondal, R. N., Kaga, Y., Hyakutake, T. and Yanase, S., Bifurcation diagram for two-dimensional steady flow and unsteady solutions in a curved square duct, Fluid Dyn. Res., Vol. **39**, pp. 413-446, 2007.

7) Nandakumar, K. and Masliyah, J. H., Swirling flow and heat transfer in coiled and twisted pipes. Advanced Transport Process, Vol. **4**, 49–112, 1986.

8) Winters, K. H., A bifurcation study of laminar flow in a curved tube of rectangular cross-section, Journal of Fluid Mechanics, Vol. **180**, pp. 343–369, 1987.

9) Yanase, S. and Nishiyama, K., On the bifurcation of laminar flows through a curved rectangular tube, Journal of the Physical Society of Japan, Vol. **57**, pp. 3790-3795, 1988.

10) Yanase, S., Mondal, R. N., Kaga, Y. and Yamamoto, K., Transition from steady to chaotic states of isothermal and non-isothermal flows through a curved rectangular duct, Journal of the Physical Society of Japan, Vol. **74(1)**, pp. 345–358, 2005.